EMPIRICAL DISTRIBUTION MODELS FOR SLENDERNESS AND ASPECT RATIOS OF CORE PARTICLES OF PARTICULATE WOOD COMPOSITES

Emmanuel K. Sackey†
PhD Candidate

*Gregory D. Smith**†
Associate Professor
Department of Wood Science
2935-2424 Main Mall
The University of British Columbia
Vancouver, BC, Canada V6T 1Z4

(Received March 2009)

Abstract. Particle geometry was characterized for particleboard furnish prepared through hydrolysis of finished commercial particleboard procured from six Canadian plants. Particles samples were screened into seven particle size classes. Particles retained on 0.5-mm mesh were considered core particles and further partitioned into core-fine, medium, and coarse. Individual particles were then randomly selected for geometrical characterization and distribution fitting. About 80% of all screened particles by mass were between mesh sizes of 0.5 and 2 mm. There were significant differences in percentage screen masses of all particle sizes between plants. Masses of particle size greater than 1 mm of panels from two plants were significantly higher than the rest (0.05 α-level), whereas another plant had the highest mass of particle sizes retained on the 2-mm mesh. Particles retained on the 1-mm mesh showed the largest percentage mass variation among all plants. It was found that aspect ratio was a better geometrical indicator for predicting screw withdrawal resistance than any of the absolute dimensions, and increase in core-fine particles increases internal bond strength. Based on maximum likelihood and Akaike's Information Criterion, a log normal distribution was the best fit for all geometrical descriptors of most particle types; gamma and two-parameter Weibull were better fits for length and aspect ratio for most medium particles with gamma being the better of the two.

Keywords: Akaike's Information Criterion, aspect ratio, core particles, particle size distribution, goodness of fit, maximum likelihood, particleboard, slenderness ratio.

INTRODUCTION

Physical and mechanical properties of wood composite products are dependent on the properties of the individual constituents, the manufacturing process, and the resulting structure from those constituents. Earlier studies on particleboard have suggested that length-to-thickness ratio, or slenderness ratio (SR), is a better indicator of the effect of particle shape on modulus of rupture (MOR) than the individual dimension. Increasing length to width ratio, or aspect ratio (AR), reduces MOR but increases screw withdrawal resistance (SWR) (Post 1961; Kusian 1968; Shuler and Kelly 1976; Lehmann 1974; Lin et al 2002). However, the interrelationship among particle size distribution, particle descriptors (AR and SR), compaction ratio, and mat compression has not been fully investigated.

Particleboard and flakeboard furnish have traditionally been characterized by screen fractionation and manual caliper measurement (Geimer et al 1999). Although caliper measurement is a direct method, it is a tedious and labor-intensive process for large particle numbers. However, it is very useful for smaller samples in a laboratory setting for analysis of particle dimensions and distributions. Geimer and Link (1988) used a sonic digitizer and micrometer to characterize flakeboard furnish. An image analysis (IA)

* Corresponding author: greg.smith@ubc.ca
† SWST member

instrument, the Cambridge Quantinet 970, was also used by Geimer et al (1999) to measure the dimensions of individual flakes. Currently, IA systems consist of a microscope, a CCD camera, a computer, and IA software. These systems have the advantage of shorter processing times and online automated measurements for relatively larger amounts of particle furnish. Nevertheless, the IA technique only quantifies the shape of the projected area of particles on a two-dimensional plane (Allen 1981). Particles tend to fall onto a horizontal surface with their widest face parallel to that surface and, as a result, IA measurements overestimate the true particle size. As such, automated measurement of SRs requires a different measuring technique. Recently, particle analysis systems based on laser diffraction (LD) technology has become available and popular (Khalili et al 2002; Li et al 2005). However, LD does not measure individual particles and one must have prior morphological information of the particles such as shape or size to correctly interpret LD results (Kelly et al 2006).

Studies of distribution models in the wood products sector have used normal, log normal, and the Erlang family of distributions to characterize fiber length distributions (Yan 1975; Kropholler and Sampson 2001). In an earlier study Geimer et al (1999) systematically characterized flakeboard furnish using geometrical descriptors and cumulative distribution curves, and panel properties were modeled using these geometrical descriptors. Lu et al (2007) recently used the Weibull and log normal models for fibers of medium-density fiberboard and core particleboard furnish. They found that the log normal was the better fit for short fibers, whereas the Weibull was the better fit for long fibers (α = 0.05). In a recent study, Cao and Wu (2007) used mixture and segmented distributions to describe wood fiber and particle length. It must be noted that the number of particle samples for the study by Lu et al (2007) was limited to two 100-g bags of particles from a single source and those of Cao and Wu (2007) were from two different sources. In hammermilled particleboard furnish, in which there is a naturally wide distribution, the fitted distribution models in those studies may not describe particles from a larger number of sources. Most of these models have focused on characterizing fiber length with the exception of Geimer et al (1999), who also examined flakeboard furnish. Because fibers are more cylindrical and needle-like compared with irregular, chunky, 3D particles, these models may not be applicable to particleboard furnish particles. Thus, there is a knowledge gap in the literature concerning the most appropriate distribution models for describing the SRs and ARs of particleboard furnish. This study proposes to develop empirical distribution models to describe the three most important particle geometry descriptors, i.e., length, SR, and AR, and correlate these to the mechanical properties of particulate wood composite panels. The main objectives are to 1) characterize the particle geometry of the core furnish in particleboard in terms of length, width, thickness, SR, and AR and relate them to panel properties; and 2) develop distribution models for length, SR, and AR of core particles for commercial particleboard furnish.

EXPERIMENTAL PROCEDURE

Particle Preparation

The source for the particles used in the study was thickness swell (TS) samples from an earlier study by Semple et al (2005). Three TS samples from three different panels were procured from each of six different particleboard plants across Canada for a total of 54 samples. The particles in each sample were separated by cooking each sample in water in a pressure vessel for 30 min to hydrolyze and dissolve the urea resin from the furnish particles. The separated particles were then filtered using a 150-μm mesh-opening sieve to remove water. The small mesh size sieve was chosen to minimize the number of small particles from being washed out of the wet furnish; however, the loss of the very fine wood flour was unavoidable. The wet particles were dried at 70°C for 1.5 h with interval stirring of the particles every 15 min to avoid agglomeration.

Dried samples were then conditioned at 65% RH and 20°C for 2 wk and bagged by plant. An issue with this process is that the original particle dimensions before their incorporation into the panel may be affected by the hysteresis that occurs in desorption process when the furnish was rewetted and then redried. Some particles might also have collapsed cell walls during hot pressing and not reach their original size (Mahoney 1980; Wolcott et al 1994). Because this is a comparative study of panels from different plants, this will be present in all samples regardless of plant.

Particle Screening, Classification, and Dimensions

The MC of 200-g samples taken from each bag was measured and recorded. Particles were screened with a Ro-Tap (Model RX 29) sieve shaker into seven different size classes as shown in Table 1. The mesh size range was selected to separate face from core furnish and to obtain more size classes within the core particles. The mesh sizes used here were similar to those used in the production of multilayer particleboard (Maloney 1970; Eusebio and Generalla 1983).

Although particle size classification differs from study to study, the industry usually divides particleboard furnish into surface fines for panel faces and coarse particles for the core. For this study, particles that passed through a 0.5-mm mesh were considered to be surface fines and those remaining on the screen as core particles. The core particles were further divided into core-fine (>0.5 mm), medium (>1 mm), and coarse (>2 mm) particles (Sackey et al 2008).

Table 1. *Mesh sizes used for particle classification.*

ASTM sieve number	Tyler mesh type	Sieve opening (mm)
5	5	4.00
10	9	2.00
18	16	1.00
35	32	0.50
60	60	0.25
120	115	0.125

Particle dimensions were measured manually using digital calipers.

The dimensions (length, width, and thickness) of 200 and 300 randomly selected particles for medium and coarse size classes, respectively, were measured and recorded for each panel from each plant. For the core-fine particles, the sample size from a replicate panel was reduced to 40 particles because preliminary particle size measurements indicated negligible variation between particles from various plants. Sample size for particle dimensions from each source was, therefore, 120, 600, and 900 for core-fine, medium, and coarse particles, respectively, making a total of 1620 particles per particleboard plant.

Data Analysis

The mass of the different particle size classes was measured and their mass percentage computed. Particle mass fraction in each size class was treated separately with a one-way analysis of variance and the plant means were compared with Tukey multiple comparison test to identify significant differences between the means.

Wide variation was observed in the size and shape of particles, especially for the medium and coarse core particles. Because all the histograms were right-skewed and zero-bound, they were fit using two-parameter log normal and Weibull distributions. These distributions can take a wide array of shapes and have been used to fit naturally occurring observations and wood fibers (Lu et al 2007). The log normal with a heavy right tail and Weibull with a heavy left tail can be considered complementary and convenient for this work because they can fit the natural variability of the particles with extremely low and high values (Meeker and Escobar 1998; Law and Kelton 2000).

The random variable X has a log normal distribution, if $Y = \ln X$ follows a normal distribution with a standard deviation σ (also called the scale parameter) greater than zero. The log normal distribution has a probability density function (PDF) as follows:

$$f(x)=\frac{1}{x\sigma\sqrt{2\pi}}\exp\left[-\frac{(\ln x-\mu^2)}{2\sigma^2}\right] \text{ for } x\geq 0$$
$$=0 \text{ for } x\leq 0 \quad (1)$$

The log normal cumulative distribution function (CDF) can be expressed in terms of the normal CDF Φ (z), where Z = (X − μ)/σ. For $x \geq 0$, the CDF is:

$$F(x;\mu,\sigma)=\Phi\left(\frac{\ln x-\mu}{\sigma}\right) \quad \text{for } x>0$$
$$=0 \quad \text{for } x\leq 0 \quad (2)$$

The CDF of Weibull distribution has the form:

$$F(x;\beta,\alpha)=1-\exp[-(x/\alpha)^{\beta}] \quad \text{for } x\geq 0$$
$$=0 \quad \text{for } x\leq 0 \quad (3)$$

where α and β are the scale and shape parameters, respectively, and are positive numbers (Stanford and Vardeman 1994). The PDF can be obtained as a derivative of $F(x; \beta, \alpha)$, which can be expressed as:

$$f(x;\beta,\alpha)=\beta\alpha^{-\beta}x^{\beta-1}\exp[-(x/\alpha)^{\beta}] \quad \text{for } x\geq 0$$
$$=0 \quad \text{for } x\leq 0 \quad (4)$$

The observations were also fit to the gamma distribution, which can accommodate variables that are highly skewed. The form of the PDF, which can be expressed in terms of the gamma function (Γ) parameterized in terms of a shape parameter k and scale parameter $\lambda - 1$, is as follows:

$$f(x;k,\lambda)=\frac{\lambda(\lambda x)^{k-1}e^{-\lambda x}}{\Gamma(k)} \text{ for } x>0 \text{ and } k,\ \lambda>0 \quad (5)$$

The CDF for the incomplete gamma function is expressed as:

$$F(k,x)=\frac{1}{\Gamma(k)}\int_0^x u^{k-1}e^{-u}du \quad (6)$$

where $\Gamma(x)=\int t^{x-1}e^{-t}dt$ (Lawless 2003). All of these distributions have two parameters with the location or threshold parameter of the gamma distribution set to zero. Goodness-of-fit test for significance of the distribution fits was performed using Anderson-Darling (AD) and Kolgomorov-Smirnov (KS) tests. The AD test procedure compares the observed with a theoretical CDF and is dependent on the actual distribution being tested. The KS test is based on the vertical difference between theoretical and empirical CDFs (EasyFit Software 2009). The AD test gives more weight to the tails of a distribution compared with the KS test. Because the differences in the observations between plants may be more pronounced at the tails, the interpretation of the results were based on AD test results.

RESULTS AND DISCUSSION

Sieve Screen Weight Data Analysis

The mean weight percentage of each particle size class for each plant is given in Table 2. Overall, 80% of particles screened remained on the 0.5-, 1-, and 2-mm meshes with most particles, 30 – 35% of the total particle mass, retained on the 1-mm screen. According to discussions with plant personnel, typical industrial surface furnish passing through a 0.75-mm mesh constitutes about 48% of the total furnish mass (Besselt 2005). These addition rates were similar to those used in this study, ie particles passing through 1-mm mesh were 40 – 53% for all plants. The means of particle mass percentages are plotted in Fig 1. Although the shapes of the distributions were similar, there were wide differences in the screen size masses be-

Table 2. *Particle mean mass on each mesh size.*

	Mass percentage of each mesh size by plant					
Mesh size (mm)*	A	B	C	D	E	F
−0.125	0.45	1.41	2.51	2.10	2.06	2.12
+0.125	1.57	2.65	5.05	4.32	5.04	4.02
+0.250	10.67	11.00	14.93	14.57	15.63	12.54
+0.500	29.06	32.60	30.15	29.12	25.02	21.83
+1.000	37.46	36.44	30.94	32.51	32.10	31.19
+2.000	18.23	14.68	15.05	16.93	19.69	22.81
+4.000	2.64	1.20	1.40	0.45	0.47	5.50

* Mesh size opening: + indicates particles retained on the mesh size and − indicates particle passing through the mesh size. Each mean is the result of n = 9 sample bags with each bag containing 200 g furnish.

tween plants for the 0.5-, 1-, and 2-mm mesh sizes. There were statistically significant differences in mass percentages between plants for all particle sizes. However, the differences between plants were lower for particles passing through the 0.5-mm and those remaining on the 4-mm meshes. The Tukey multiple comparison test at the 0.05 α-level indicates a significantly higher mass of the 1-mm particle size class in panels from plants A and B, whereas plant F had the highest amount of particle sizes above the 2-mm mesh.

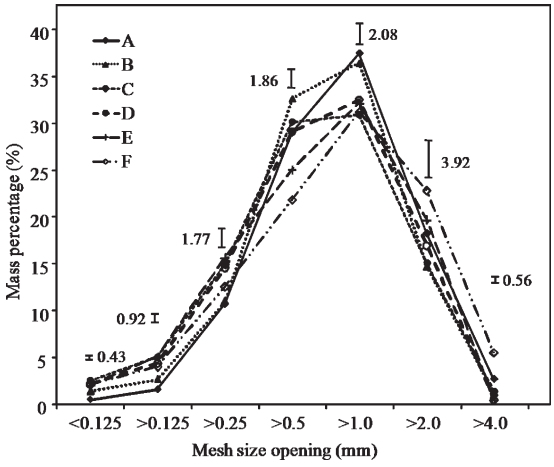

Figure 1. Distribution of mean particle mass as a percentage of total particle mass for each particle size class; least significant difference bars are given for comparison of the mean particles size from each plant for that size class.

Geometrical Descriptors and Their Effect on Panel Strength

Means of particle geometry with their calculated AR and SR and projected surface area are listed on Table 3. There were significant differences ($p < 0.0001$) between plants for all geometrical descriptors with the exception of width for the medium particles. It was also observed that the finer particles had smaller size differences between plants, which was similar to the observation for mass percentages. The mean length and width of the core-fine particles from plant F were higher than those of plant A;

Table 3. *Comparison of the means of geometrical descriptors of the core-fine, medium, and coarse core particles.*

	Furnish source (plant)					
Particle class	A	B	C	D	E	F
Length (mm)						
Core-fine	3.96 a	1.98 d	3.66 a,b	2.88 c	3.14 c	4.05 a
Medium	9.44 a	5.97 b	5.78 b	7.03 a	7.57 a	8.03 a
Coarse	12.26 a	8.67 c	9.16 b	9.64 b	9.27 b	10.53 a
Width (mm)						
Core-fine	0.90 b,c	0.97 a,b	1.00 a	0.97 a,b	0.85 c	0.92 a,b,c
Medium	1.84 a	1.88 a	1.85 a	1.91 a	1.86 a	1.91 a
Coarse	3.79 c	4.26 a,b	4.17 b	3.78 c	3.62 d	4.38 a
Thickness (mm)						
Core-fine	0.28 b	0.27 b	0.36 a	0.28 b	0.23 b	0.25 b
Medium	0.74 a	0.59 b	0.70 a	0.74 a	0.74 a	0.67 a
Coarse	1.12 b	1.11 b	1.22 a	1.41 a	1.29 a	1.15 b
Aspect ratio (−)						
Core-fine	4.63 a,b	2.21 c	4.28 a	3.26 b	4.09 a,b	4.84 a
Medium	5.64 a	3.43 e	3.62 d,e	4.00 c,d	4.34 c	4.72 b
Coarse	3.80 a	2.48 e	2.71 d	3.04 b	2.95 b	2.84 c
Slenderness (−)						
Core-fine	16.45 a,b	10.09 c	12.14 c	13.22 b,c	19.81 a	20.42 a
Medium	15.02 a	12.55 b	14.71 b,c	11.82 c	12.05 b,c	14.23 a
Coarse	12.13 a	8.58 b	8.25 b	7.69 b	8.53 c	10.38 a
Surface area (mm^2)						
Core-fine	3.48 a	1.92 c	3.40 a	2.71 b	2.57 b	3.65 a
Medium	17.42 a	11.16 d	11.59 d	13.30 c	14.07 b,c	14.95 b
Coarse	47.30 a	37.02 b,c	38.62 b	38.10 b,c	35.23 c	47.86 a

Note: Means are not significantly different if the letter beside them is the same. n = 120 (core-fine); n = 600 (medium); and n = 900 (coarse) for each mean.

consequently, the AR, SR, and surface area followed a similar trend. However, core-fine particles were less in the core and hence have minimal effect on the mechanical properties compared with the medium and coarse particles. For the medium and coarse particles, plant A had significantly longer, but relatively narrow, particles compared with all other plants, resulting in higher AR, SR, and surface area for the medium and coarse particles. Because particle length determines the number of interparticle contact points of a particle with adjacent ones, the longer the particle, the better the inherent particle strength contributes to the overall consolidated panel strength (Marra 1954), as demonstrated by the particles from plant A (see Table 4).

The mechanical properties of the panels from which the particles were derived have been reported by Semple et al (2005); hence, only the likely effect of particle geometry on the mechanical properties are discussed. According to Heebink and Hann (1959) and Post (1961), increasing SR increases flexural properties and these were shown in plant A for modulus of elasticity (MOE) and modulus of rupture and in plant F for MOE. The larger surface area of the particles from plant A and F were likely to have resulted in more bonds with adjacent particles, thus increasing their ability to transfer stress. Although increasing AR decreases flexural properties, this was not seen in panels from plant A, because the high AR was likely offset by the very high SR of those particles. The higher internal bond (IB) and edge SWR from plant A may be from the lower thickness and width of particles producing a better packing efficiency. The high surface area also increases the area available for resin coverage. Coarse and medium particles from plant B, which were relatively short, wide, and thin, had lower AR, SR, and surface area. With the smaller surface area, the particles have less opportunity for bonding with adjacent particles and likely led to the lower mechanical properties of those boards (Semple et al 2005).

Relationship Between Properties and Particle Descriptors of Particleboard Core

Figure 2 shows the relationship between the mechanical properties of the core board structure and the AR and SR of particleboard furnish. There is a general positive trend between the properties and the descriptors. Figure 2a shows a relatively high correlation between SWR and AR of the medium and coarse particles with $R^2 = 0.82$ and 0.84, respectively, confirming the results of Lehmann (1974) and Lin et al (2002). Particles with higher AR tend to be chunky having more wood substance and form particle stacks from overlaps of adjacent particles and present a better grip for screws and higher resistance during withdrawal. Higher AR also offers a higher surface area for resin coverage, which assists in bonding. Although higher SR leads to more particle overlaps and stacking, the particles are too thin with less material available for the screw to grip, consequently leading to lower

Table 4. *Means of mechanical properties for panels from plants A to F.*

Property	Plants					
	A	B	C	D	E	F
Density (kg/m^3)	681	707	702	658	647	648
IB (MPa)	0.7	0.4	0.7	0.6	0.6	0.6
Face SWR-A (N)	1098	837	1020	1035	1016	950
Face SWR-B (N)	1166	883	1031	1076	1026	992
Edge SWR (N)	973	634	776	733	771	790
MOR $\parallel$ (MPa)	16.0	13.5	14.7	16.6	12.3	13.4
MOR $\perp$ (MPa)	15.0	12.6	14.2	15.3	12.2	13.0
MOE $\parallel$ (GPa)	3.1	2.3	2.6	3.0	2.6	2.8
MOE $\perp$ (GPa)	2.8	2.2	2.4	2.8	2.4	2.7

Adapted and modified from Semple et al (2005).
SWR = screw withdrawal resistance; MOR = modulus of rupture; MOE = modulus of elasticity.

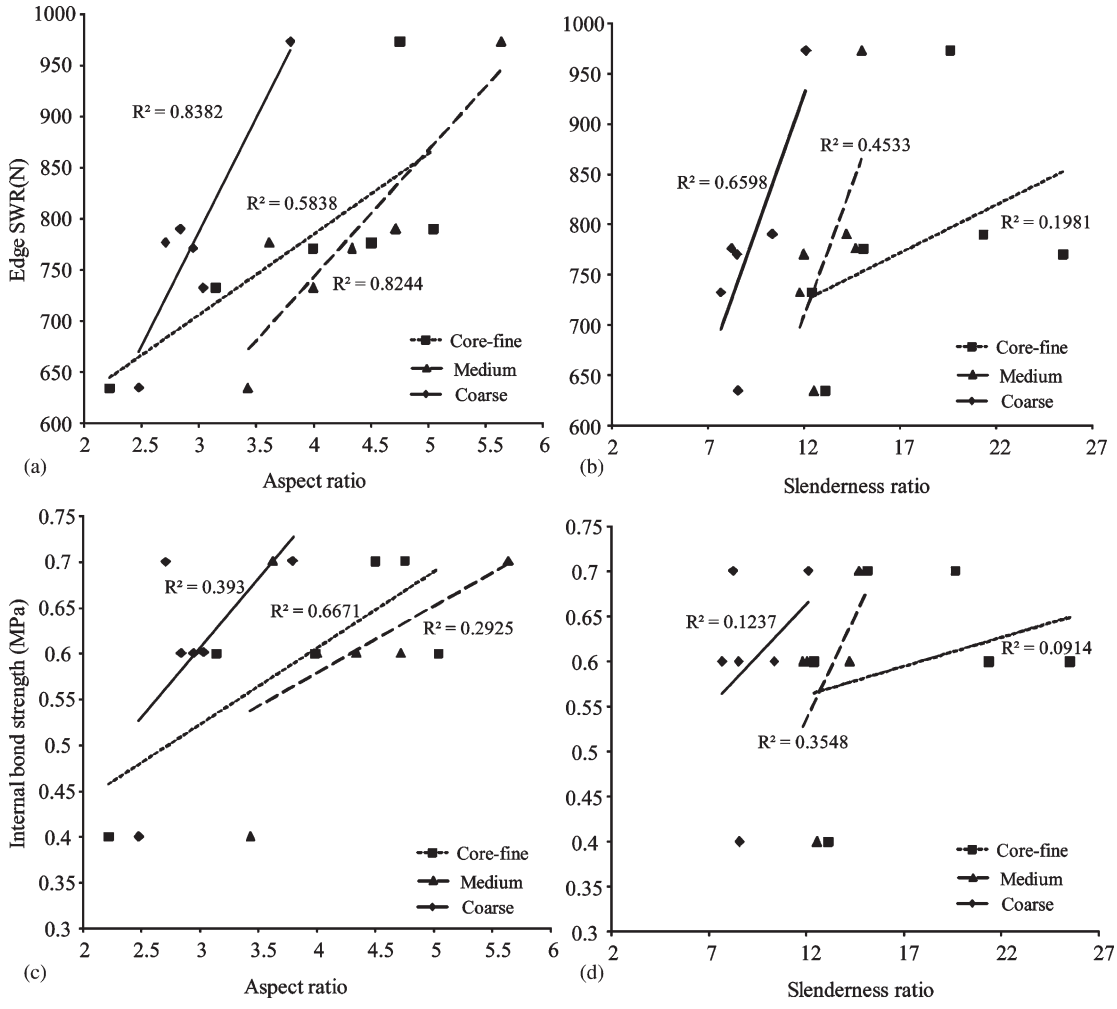

Figure 2. Relationship between mechanical properties [edge screw withdrawal resistance (SWR) and internal bond (IB) strength] and geometrical descriptors (aspect ratio and slenderness ratio) for core-fine, medium, and coarse particles of particleboard core. The upper row, (a) and (b), is edge SWR and the lower row, (b) and (c), is IB strength.

R^2 of 0.45 and 0.66 with SWR for medium and coarse particles. Relative to SWR, the correlation between IB and AR was very low with the exception of AR of core-fine particles, which had an R^2 of 0.67. The core-fines fill the voids within and between the coarse and medium particles, increasing the bonds formed; hence the higher the fines in the core, the higher the IB strength (Nemli 2003; Kakaras and Papadopoulos 2004; Sackey et al 2008). Like in earlier studies, IB strength did not show a good correlation with SR of any of the particle sizes. (Note that the flexural properties of the panel were not considered because they are influenced mainly by the face structure of the panel.)

Particle Geometrical Descriptors and Their Distribution

The histograms for particle length and AR and SR are shown in Fig 3 and are overlaid with the best-fitting distribution models from the log normal, gamma, and Weibull family of distributions. The maximum likelihood method of the

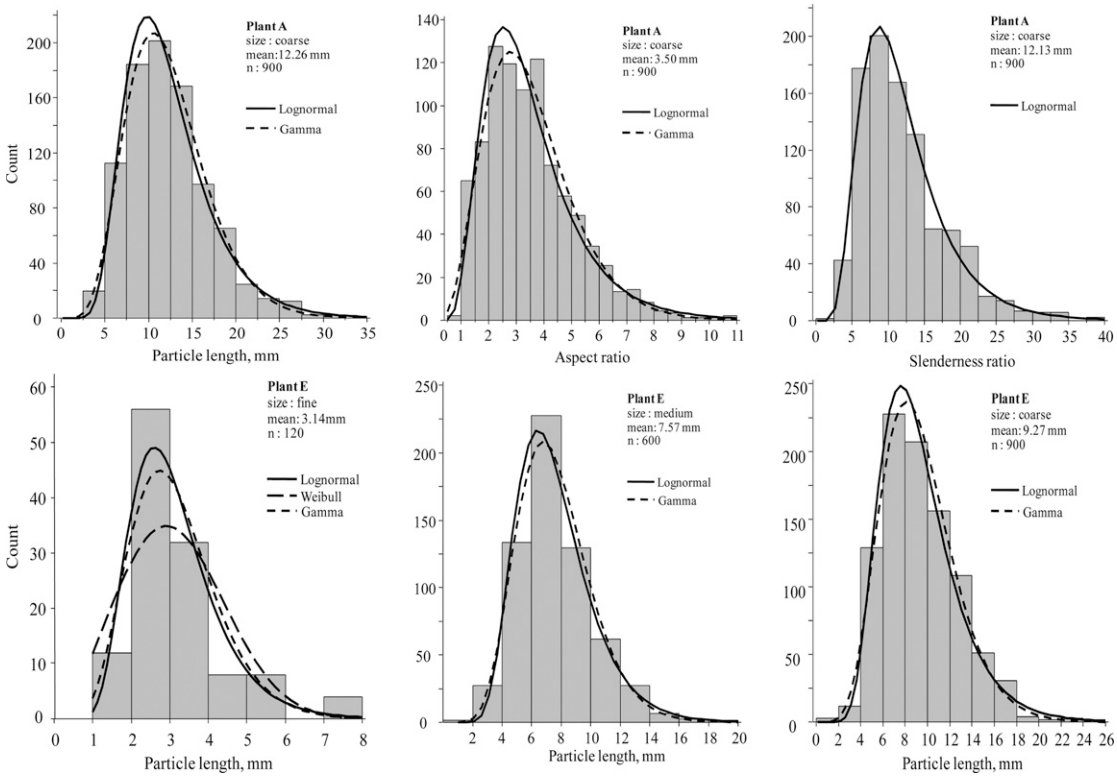

Figure 3. Typical histograms of the observations overlaid with best fit distribution. Upper row shows distribution of particle length and aspect and slenderness ratios of the coarse particles from plant A, and the lower row shows distribution of particle length of core-fine, medium, and coarse particles from plant E.

reliability procedure in SAS®9.1 (SAS 2002) and the Akaike's Information Criterion (AIC) were used to determine the best-fitting distribution for each plant's particle data set. The AIC, which is an extension of the maximum likelihood principle, provides a quantitative measure for selecting the best distribution model for the data set and can be expressed as:

$$\mathrm{AIC} = -2\log\left(\mathrm{L}(\hat{\theta}|\mathrm{data})\right) + 2\mathrm{k} \qquad (7)$$

where $\mathrm{L}(\hat{\theta})$ is the likelihood function evaluated at the maximum likelihood estimator $\hat{\theta}$ and k is the number of parameters (Akaike 1973; Bozdogan 2000; Burnham and Anderson 2004). The shape and scale parameter estimates and their maximum log (likelihood) (ML) values for the lognormal and Weibull models for AR and SR of coarse particles are listed in Table 5. The distribution with the highest ML value is the best fit. Comparing the ML values from the log normal and Weibull distributions (Table 6), the log normal was consistently a better fit for the three descriptors of particles from most plants than the Weibull distribution. The Weibull distribution was a better model only for the length and AR of the medium particles from plant D shown in Table 6.

Log likelihood values for log normal, gamma, and two-Weibull distributions and their parameter estimates were performed using JMP (2008) software. However, to allow for comparison with more than two-parameter distributions in the future and other studies, AICc (corrected AIC) listed in Table 6 were computed and used in ranking the distributions; the lower an AIC value, the better the distribution fit. How well a distribution fits a descriptor of a particle class from a plant was ranked 1, 2, or 3 for best,

Table 5. *Model parameters of aspect and slenderness ratios for coarse particles.*

		Log normal			Weibull		
	Plant	ML	Scale (σ)	Shape (μ)	ML	Scale (α)	Shape (β)
Aspect ratio	A	−598.440	1.1468	0.4707	−629.397	3.9647	2.2910
	B	−519.653	0.6882	0.4313	−662.568	2.4956	2.0887
	C	−547.326	0.7690	0.4448	−634.361	2.7063	2.2234
	D	−499.077	0.9868	0.4215	−537.753	3.3027	2.5320
	E	−523.653	0.9711	0.4332	−569.468	3.2714	2.4289
	F	−564.131	0.8503	0.4531	−644.940	2.9443	2.1999
Slenderness ratio	A	−596.391	2.3849	0.4697	−674.213	13.7351	2.1103
	B	−466.085	2.0627	0.4064	−592.133	9.6986	2.2584
	C	−492.370	2.0197	0.4184	−612.834	9.3291	2.2011
	D	−400.301	1.9987	0.3777	−591.334	8.9863	2.1543
	E	−391.377	2.0258	0.4229	−532.979	9.4672	1.9702
	F	−621.188	2.2166	0.4828	−746.684	11.7654	1.9025

ML + maximum log (likelihood).

Table 6. *AICc values of aspect and slenderness ratios for coarse particles.*

	Aspect ratio(AR)			Slenderness ratio (SR)		
Plant	Log normal	Gamma	Weibull	Log normal	Gamma	Weibull
A	*3265.43*	***3263.27***	3327.26	***5489.73***	*5527.02*	5645.34
B	***2282.16***	*2385.63*	2568.03	***4649.07***	*4719.43*	4901.20
C	***2482.80***	*2536.36*	2656.86	***4624.03***	*4687.04*	4865.06
D	***2716.01***	*2723.55*	2798.75	***4535.70***	*4645.24*	4708.72
E	***2798.63***	*2819.90*	2916.56	***4761.80***	*4910.30*	5149.88
F	***2662.93***	2824.62	*2709.93*	***5236.39***	*5324.98*	5487.34

Note: Bold italics denote best fit distributions, italics are next best and the least fit are the distributions in regular font.

better, or good fit, respectively. For example, for the AR of plant A, the gamma distribution was assigned a value of 1, the log normal a value of 2, and the Weibull a value of 3. This was repeated for all plants and the total score was computed for each distribution; the scores range from 6 to 18 for each descriptor. The distribution with the lowest ranking score for all plants indicates the best model for a particular descriptor. Generally, two-parameter log normal distribution provided the best fit model for SR in all particle size classes. The AIC scores also showed that the two-parameter Weibull was the least fit for all three descriptors. This is contrary to the results from Lu et al (2007) who found the Weibull distribution to be the best fit for the core particles of particleboard. This discrepancy may be from lower variability in their samples, which were drawn from only one source. Care must be taken in comparing the two studies, however, because there was a further partitioning of the core particles in this study, which was not the case with the study of Lu et al (2007). It must be noted that the whole furnish characterization followed similar distribution patterns as the partitioned furnish. Length and AR of the core-fine particles are best fit by a log normal distribution, model.

Goodness-of-Fit Tests

In the goodness-of-fit test, the null hypothesis, H_O, is that the data follows the log normal (or Weibull or gamma) distribution and the alternate hypothesis, H_A, is that the data do not follow the specified distribution at $\alpha = 0.05$. In Table 7, L, G, and W represent cases in which the distribution of log normal, gamma, or Weibull, respectively, fits length, AR, and SR from a particular plant. Although both AD and KS tests were used in all instances, there were few

Table 7. *Goodness-of-fit test for the distribution models for length, aspect ratios, and slenderness ratios of core-fine, medium, and coarse industrial particles.*

	Length			Aspect ratio			Slenderness ratio		
Plant	Core-fine	Medium	Coarse	Core-fine	Medium	Coarse	Core-fine	Medium	Coarse
A	L	L, G	L, G	L, G, W	L	L, G	L, G	L	L
B	nf	L, G	nf	L	L	nf	L	L	L
C	nf	L, G, W^{KS}	L	nf	L, G, W^{KS}	L^{KS}	nf	nf	L
D	L, G	G, W	L, G	L	G, W	L, G	L^{KS}	nf	L
E	L, G	L, G	L, G	L^{AD}	L, G	L, G	nf	L^{AD}	L^{KS}
F	L, G	G, W	L	L, G	L	L	L, G, W^{KS}	L	L

L, G, W = fail to reject HO, data from a log normal, gamma, or Weibull distribution respectively, whereas nf indicates no fit; KS = Kolmogorov Smirnov test; AD = Anderson-Darling.

cases in which only one of these tests was significant and it is indicated by a superscript AD or KS.

Generally, the log normal distribution was the best fit for most of the descriptors, particularly for the medium particles, because most of the particle distributions have a heavier right tail. Particle length and AR of the medium particles from plant D were best fit with the gamma and Weibull models, whereas the log normal model was not a good fit. These particles were relatively short (Table 3) and hence weighted toward zero (Meeker and Escobar 1998; Lu et al 2007). Unlike Lu et al (2007), all three two-parameter distribution models were rejected for some particles from plants B, C, D, and E with the greater percentage from plants B and C, which are inadvertently sister plants in two different locations. It must be noted that the gamma family of distributions, which has been the least used distribution for modeling wood particles and fibers, was a better fit for most particle size classes than the two-parameter Weibull distribution. The lack of fit for most of the distributions for SR for medium and coarse particles may be from the lower variability found in particle thicknesses, making the distribution pattern of SR, to some extent, similar to that of the length distribution.

The results of this investigation suggest that properties of conventional particleboard panels on the market can be correlated with the length, AR, and SR of the hydrolyzed particles. Knowledge of the continuous particle distribution models obtained opens avenues for further work in obtaining optimal particle packing efficiencies in particulate wood composites. The distribution models should make possible the manipulation of particle geometries to improve strength properties. Distribution models will also assist in formulating particle distributions that will increase or decrease porosity of a panel mat, which affects permeability during hot pressing and may lead to particle mixtures that reduce degassing times. Mat compression behavior can also be influenced with the knowledge of particle size distribution and their variability. For instance, from a log normal distribution model, the thickest particles in the upper 5% in the core of the particle mat, which leads to higher mat compression and consequent compressive failure, can be removed by lowering the heavy right tail of the distribution.

CONCLUSIONS

Within the confines of this study, the following conclusions can be drawn. Overall, about 80% of the total mass of particles was retained on the 0.5-, 1-, and 2-mm meshes with about 35% of the total mass of particles retained on the 1-mm mesh alone. There was a significant difference in furnish mass percentage among all six plants for all particle sizes. Less variation was found between percentage mass of fine particles (<0.5-mm mesh) and between percentage mass of the largest (>4 mm) particles than the mid-range sizes. Particle AR is a better material predictor for screw withdrawal resistance of particulate wood composites than absolute geometrical dimensions and increase in core-fine

particles increase internal bond strength. The log normal distribution provided the best fit for length, SR, and AR for all particle types (core-fine, medium, and coarse) for the core furnish. Gamma distribution also provides a good model fit for length, AR, and SR for the core-fine, medium, and coarse particles compared with the Weibull. From this study, it can be concluded that log normal and gamma distributions are good distribution models for characterizing the SR and AR of irregular particulate wood material.

ACKNOWLEDMENTS

We gratefully acknowledge the funding support of Natural Resources Canada and extend our thanks to Dr. Kate Semple for her invaluable proofreading and input.

REFERENCES

Akaike H (1973) Information theory and an extension of the maximum likelihood principle. Pages 267 – 281 *in* BN Petrov and F Csaki, eds. Second International Symposium on Information Theory, Academiai Kiado, Budapest.

Allen T (1981) Particle size measurement. 3rd ed. Chapman and Hall Ltd., New York, NY.

Besselt N (2005) Technical discussion at NewPro particleboard plant in Wahnam AB with the Technical Director on 9 May 2005.

Bozdogan H (2000) Akaike's information criterion and recent developments in information complexity. J Math Psychol 44(1):62 – 91.

Burnham KP, Anderson DR (2004) Multimodel inference: Understanding AIC and BIC in model selection. Colorado Cooperative Fish and Wildlife Research Unit (USGS-BRD). Sociological Methods and Research 33(2): 261 – 304.

Cao QV, Wu Q (2007) Characterizing wood fiber and particle length with a mixture distribution and segmented distribution. Holzforschung 61:124 – 130.

EasyFit Software (2009) EasyFit Help, goodness of fit. MathWave Technologies, www.mathwave.com.

Eusebio GA, Generalla NC (1983) Effect of particle resin adhesive distribution in particleboard manufacture of Kaatoan Bangkal [Anthocephalus chinensis (Lam.) Rich. Ex Walp.]. FPRDI Journal Vol 12(3 – 4):12 – 19.

Geimer RL, Evans JW, Setiabudi D (1999) Flake furnish characterization—Modeling board properties with geometric descriptors. Res Pap FPL-RP-577. USDA Forest Service, Forest Prod Lab, Madison, WI. 36 pp.

———, Link CL (1988) Flake classification by image analysis Res. Pap. FPL-RP-486. USDA Forest Service, Forest Prod Lab, Madison, WI. 25 pp.

Heebink BG, Hann RA (1959) How wax and particle shape affect stability and strength of oak particleboards. For Prod J 9(7):197 – 203.

JMP (2008) JMP 8 Statistical Discovery Software. SAS Institute Inc. Cary, NC.

Kakaras IA, Papadopoulos AN (2004) The effects of drying temperature of wood chips upon the internal bond strength of particleboard. J Inst Wood Sci 16(5):277 – 279.

Kelly RN, DiSante JK, Stranzl E, Kazanjian JA, Bowen P, Matsuyama T, Gabas N (2006) Graphical comparison of image analysis and laser diffraction particle size analysis data obtained from the measurements of nonspherical particle systems. AAPS PharmSciTech 7(3):E1 – E14.

Khalili MA, Roricht WL, Luke LSY (2002) An investigation to determine the precision for measuring particle size distribution by laser diffraction. World Congress on Particle Technology 4, 21 – 25 July 2002, Sydney, Australia. Paper no. 111.

Kropholler HW, Sampson WW (2001) The effect of fiber length distribution on suspension crowding. Pulp Paper Sci 27(9):301 – 305.

Kusian R (1968) Model investigations about the influence of particle size on structural and strength properties of particle materials. II. Experimental investigations. Holztechnologie 9(4):241 – 248.

Law AM, Kelton WD (2000) Simulation modeling and analysis. 3rd ed. McGraw-Hill Publishers, New York, NY. 760 pp.

Lawless JF (2003) Statistical models and methods for lifetime data. John Wiley and Sons, Inc, Hoboken, NJ.

Lehmann WF (1974) Properties of structural particle boards. For Prod J 24(1):19 – 26.

Li M, Wilkinson D, Patchigolla K (2005) Comparison of particle size distributions measured using different techniques. Particul Sci Technol 23:265 – 284.

Lin HC, Fujimoto Y, Murase Y, Mataki Y (2002) Behaviour of acoustic emission generation during tensile tests perpendicular to the plane of particleboard II: Effects of particle sizes and moisture content of boards. J Wood Sci 48(5):374 – 379.

Lu JZ, Monlezun CJ, Wu Q, Cao QV (2007) Fitting Weibull and lognormal distributions to medium-density fiberboard fiber and wood particle length. Wood Fiber Sci 39(1):82 – 94.

Mahoney RJ (1980) Physical changes in wood particles induced by the particleboard hot pressing operation. Pages 213 – 223 *in* TM Maloney, ed. Proc 14th International Symposium on Particleboard, April 1980, Pullman, WA.

Maloney TM (1970) Resin distribution in layered particleboard. For Prod J 20(1):43 – 52.

Marra GG (1954) Discussion following article by Turner HD—Effect of particle size and shape on strength and dimensional stability of resin-bonded wood-particle panels. For Prod J 4(5):210 – 223.

Meeker WQ, Escobar LA (1998) Statistical method for reliability data. John Wiley & Sons, Inc, New York, NY.

Nemli G (2003) Effects of some manufacturing factors on the properties of particleboard manufactured from Alder (*Alnus glutinosa* subs. *Barbata*). Turk J Agric For 27: 99 – 104.

Post PW (1961) Relationship of flake size and resin content to mechanical and dimensional properties of flake board. For Prod J 11(9):34 – 37.

Sackey E, Semple K, Oh S-W, Smith GD (2008) Improving core bond strength of particleboard through particle size redistribution. Wood Fiber Sci 40(2):214 – 224.

SAS (2002) The reliability procedure. SAS/QC® user's guide. SAS Institute, Inc., Cary, NC.

Semple K, Sackey E, Park HJ, Smith GD (2005) Properties variation study of furniture grade M2 particleboard manufactured in Canada. For Prod J 55(12):117 – 124.

Shuler CE, Kelly RA (1976) Effect of flake geometry on mechanical properties of eastern spruce flake-type particleboard. For Prod J 26(6):24 – 31.

Stanford JL, Vardeman SB (1994) Statistical methods for physical science. Vol. 28. Method of experimental physics. Academic Press, San Diego, CA.

Wolcott MP, Kamke FA, Dillard DA (1994) Fundamentals aspects of wood deformation pertaining to manufacture of wood-based composites. Wood Fiber Sci 26:496 – 511.

Yan JF (1975) A method for the interpretation of fiber length classification data. TAPPI 58(8):191 – 192.